2. DATE	3. REPORT TYPE AND DATES COVERED
9/1/93	Final Report June 1992 - June 1993

4. TITLE AND SUBTITLE
Competitive dynamics and self-organization in photorefractive systems

5. FUNDING NUMBERS
N00014-91-J-1212

6. AUTHOR(S)
Dana Z. Anderson

7. PERFORMING ORGANIZATION NAME(S) AND ADDRESS(ES)
University of Colorado
Joint Institute for Laboratory Astrophysics
Campus Box 440
Boulder, Colorado 80309

8. PERFORMING ORGANIZATION REPORT NUMBER

9. SPONSORING/MONITORING AGENCY NAME(S) AND ADDRESS(ES)
Office of Naval Research
Code 412, Physics Division
Arlington, VA 22217

10. SPONSORING/MONITORING AGENCY REPORT NUMBER

11. SUPPLEMENTARY NOTES

12a. DISTRIBUTION/AVAILABILITY STATEMENT
Approved for public release; distribution unlimited.

12b. DISTRIBUTION CODE

13. ABSTRACT *(Maximum 200 words)*

Information can be manipulated and processed by a nonlinear dynamical system. This work investigates the properties of such nonlinear optical systems based upon real-time holographic materials known as photorefractive media. Our goal is to understand how and when a dynamical system can self-organize, or learn on its own to process information in a useful way. We have demonstrated systems, for example, that can separate multiple fiber optic communication channels or learn to classify incoming images. We have discovered that such self-organizing systems will exhibit a phase-transition with the information content of the input as the critical parameter. The phase-transitions are analogous to those common to thermodynamic systems. In order to better provide an analytical basis of treatment of our systems we have developed various analytical tools, in particular stability analysis tools. We have also looked at the photorefractive version of well known nonlinear dynamical problems such as the formation of hexagonal patterns in pumped photorefractive media.

14. SUBJECT TERMS	15. NUMBER OF PAGES
Nonlinear optics, nonlinear dynamics, photorefractive materials, neural networks, holography	19
	16. PRICE CODE

17. SECURITY CLASSIFICATION OF REPORT	18. SECURITY CLASSIFICATION OF THIS PAGE	19. SECURITY CLASSIFICATION OF ABSTRACT	20. LIMITATION OF ABSTRACT
Unclassified	Unclassified	Unclassified	

Competitive Dynamics and Self-Organization in Photorefractive Systems

A Final Report

ONR Grant N00014-91-J-1212

I. Overview

Research for the period June 1992 to June 1993 has encompassed several topics in competitive dynamics and self organization in photorefractive systems:

1) Stability analysis of photorefractive circuits.

2) Spatio-temporal dynamics in a photorefractive ring oscillator.

3) Transverse instability of counterpropagating beams in photorefractive media.

A short synopsis of results in each of these areas is included in the rest of this section, while additional details are given separately for each topic in the following sections.

It was demonstrated over the past several years that photorefractive ring resonators and circuits of coupled photorefractive resonators are suitable for implementing a wide variety of competitive and cooperative dynamics [1-7] including specifically, the bistable ring resonator with gain and loss [1,2], "winner-takes-all" and "voting paradox dynamics" [3], a photorefractive flip-flop [4], a ring-resonator with history dependent feedback [5], and self-organizing feature extractors that operate on frequency or time multiplexed spatial patterns [6,7]. These systems were demonstrated experimentally before a full theoretical analysis was completed. We have now completed stability analyses of the flip-flop [4], and the self-organizing feature extractor [6,7] that confirm the experimental observations. A detailed analysis of the flip-flop [27] clarifies the role of the time constants in the gain and loss media on the system stability. Analysis of a simplified model of the feature extractor [8] shows that the desired stationary state corresponding to extraction of the input patterns is stable, and all other stationary states are unstable. In the case of the feature extractor numerical analysis has been used to study the time dependence of the transition to a self-organized state, and the role of noise induced symmetry breaking in this system.

In order to study more complex self-organizing systems than the feature extractor we have moved to an investigation of a single, transversely continuous ring resonator [9]. This resonator allows for the self-organized formation of transversely continuous spatial patterns, whereas in the coupled ring resonators the complexity of the self-organized pattern is limited by the number of coupled rings. We choose to work with an imaging resonator that admits an arbitrary transverse mode as an eigenmode. In this situation, where the passive optics play only a minor role in determining the

mode structure the impact of the nonlinear elements comes to the forefront. Our initial experimental results demonstrated how photorefractive gain and loss, placed in Fourier conjugate resonator planes, induce the continuum of transverse modes to collapse into a single localized mode of near Gaussian form. Since the imaging ring has no optical axis the location of the localized mode is arbitrary, and is seen to form at any point in the transverse plane of the resonator. In fact, due to imperfect alignment of the resonator, the localized mode, or spot, is not stationary, but rather drifts in the transverse plane [10]. This phenomena appears to be unique in the field of nonlinear optics. Analytical and numerical studies of the resonator show that the rate of spot motion is directly dependent on the amount of cavity misalignment.

Part of the motivation for studying nonlinear dynamics in photorefractive systems is the possibility of implementing neuromorphic information processing systems. In this context the localized excitation in the photorefractive ring resonator represents the response of the information processing system to an input pattern (the resonator pump beam). We have investigated the response of an idealized resonator with no cavity misalignment to time multiplexed input patterns. We find from numerical simulations that input patterns with a large degree of similarity lead to resonator excitations lying close together, while dissimilar input patterns lead to resonator excitations spaced far apart. It appears therefore possible to use this resonator concept to implement a class of neural network algorithms due to Kohonen, known as topology preserving mappings [11].

While the motion of the localized excitation is interesting in its own right as an example of novel dynamical behavior, it is undesirable for implementing e.g. a topology preserving mapping that should result in a stationary output when presented with a statistically stationary input. We have therefore investigated various ways in which additional nonlinearities may be used to inhibit the motion, while still allowing the mode to form at an arbitrary position. Most of this work has been performed numerically using a 3-D simulation program that allows a wide variety of resonator configurations to be investigated. In early June 1993 we succeeded in finding a configuration, requiring one additional photorefractive crystal, that stabilizes the spot motion on the computer, despite cavity misalignments. Work is now under way to demonstrate this experimentally.

In addition to the work on photorefractive ring resonators we have studied a more traditional topic in nonlinear optics: the transverse modulational instability of counterpropagating waves. The modulational instability is well known in nonlinear optics, dating back to some Soviet work from the late 1970's [12]. The nonlinear stage of the instability results in the formation of transverse patterns, including rings, squares and hexagons, and has been observed experimentally in atomic vapors [13-15], liquid crystals [16,17], and quite recently in photorefractive media [18]. The intrinsically slow dynamics of photorefractive media which simplifies time resolved measurements, and their low thresholds, which make the strongly nonlinear stage of the instability accessible, render them well suited to further experimental investigation of these phenomena. The likelihood that photorefractive media will come to contribute to better understanding of the nonlinear aspects of pattern formation in this system motivates the theoretical analysis of the instability threshold that we have undertaken as a first step towards analyzing the nonlinear stage of the instability.

The analysis is complicated in photorefractive media by the fact that the coupling constant is in general complex, whereas it is purely real in the instantaneous Kerr media that have been the

subject of previous theoretical work. A paper describing the instability threshold condition due to the formation of transmission gratings in photorefractive media has been accepted for publication [19]. A second theoretical contribution in this area that considers the reflection grating case which was experimentally realized [18], is nearing completion [20].

II. Stability analysis of photorefractive circuits

The analytical tools necessary for detailed analysis of the stability of photorefractive circuits based on two-beam coupling can be found as an extension of the methods that were previously developed for treating a number of four-wave mixing configurations in photorefractive media [28]. The conceptual basis of the method is quite straightforward: perform a linear stability analysis about all possible stationary solutions of the circuit under consideration, in order to isolate the stable solutions. The mechanics of carrying this program out becomes involved as the complexity of the circuits increases. The analysis is lengthy because the steady state solutions almost always involve nonlinear variations of the optical fields and photorefractive index gratings. Thus the linear perturbation analysis must be performed about a nonlinear steady state.

The simplest configuration we wish to analyze is the dynamics of two beam coupling, which is described by the equations

$$\frac{\partial s}{\partial x} = gp, \qquad \frac{\partial p}{\partial x} = -g^{*}s,$$
$$\left(\tau\frac{\partial}{\partial t}+1\right)g = \frac{\Gamma}{2I_T}sp^{*} \tag{II.1}$$

where s and p are the amplitudes of the signal and pumping beams respectively, g is the amplitude of the grating, Γ is the coupling constant, $\tau \propto I_T^{-1}$ is the characteristic time constant of the medium and $I_T = |s|^2 + |p|^2$ is the sum of intensities of the interacting beams. The well known steady state solutions of Eqs.(II.1) for real coupling may be written in the form

$$|s_0|^2_{out} = |s_0|^2_{in} M, \quad |p_0|^2_{out} = |p_0|^2_{in} M\exp(-\Gamma),$$
$$M = \frac{1+r}{r+\exp(-\Gamma)}, \tag{II.2}$$

where $r = |s_0/p_0|^2_{in}$ is the input beam intensity ratio. Equations (II.2) allow for any sign of Γ. Below we will use the notation $\Gamma \equiv \Gamma_G$, $M \equiv G$ for $\Gamma > 0$ (when the signal beam experiences gain) and $\Gamma \equiv -\Gamma_L$, $M \equiv L$ for $\Gamma < 0$ (when it experiences loss).

Arbitrary complex perturbations about the steady state solution can be separated into purely real and purely imaginary contributions and their evolution can be described independently. Below we restrict ourselves to consideration of purely real perturbations, since they turn out to be more important for the analysis of the circuits considered here. The time dependent amplitudes are therefore written in the form

$$\begin{aligned} s(x,t) &= s_0(x) + \mathrm{Re}\big(\delta s(x)\exp(ft)\big), \\ p(x,t) &= p_0(x) + \mathrm{Re}\big(\delta p(x)\exp(ft)\big). \end{aligned} \tag{II.3}$$

where f is a complex frequency.

Linearizing Eqs.(II.1) with respect to δs and δp around the stationary solution (II.2) and solving the resulting equations results in a transmission matrix, that describes propagation of perturbations through a medium by coupling their input and output amplitudes

$$\begin{pmatrix} \delta s \\ \delta p \end{pmatrix}_{out} = \hat{T}^{(2)} \begin{pmatrix} \delta s \\ \delta p \end{pmatrix}_{in}, \tag{II.4}$$

where the 2 x 2 transmission matrix elements are given by the relations:

$$\begin{aligned} T_{11}^{(2)} &= \frac{\exp(\Gamma/2)}{\Delta\sqrt{M}}\left[r\exp(\Gamma/2) + \exp\left(\frac{1}{1+\tau f}(\ln M - \Gamma/2) \right) \right], \\ T_{12}^{(2)} &= \frac{\exp(\Gamma/2)}{\Delta\sqrt{M}}\sqrt{r}\left[\exp(\Gamma/2) - \exp\left(\frac{1}{1+\tau f}(\ln M - \Gamma/2) \right) \right], \\ T_{21}^{(2)} &= \frac{\exp(\Gamma/2)}{\Delta\sqrt{M}}\sqrt{r}\left[1 - \exp\left(\Gamma/2 + \frac{1}{1+\tau f}(\ln M - \Gamma/2) \right) \right], \\ T_{22}^{(2)} &= \frac{\exp(\Gamma/2)}{\Delta\sqrt{M}}\left[1 + r\exp\left(\Gamma/2 + \frac{1}{1+\tau f}(\ln M - \Gamma/2) \right) \right], \\ \Delta &= 1 + r\exp(\Gamma). \end{aligned} \tag{II.5}$$

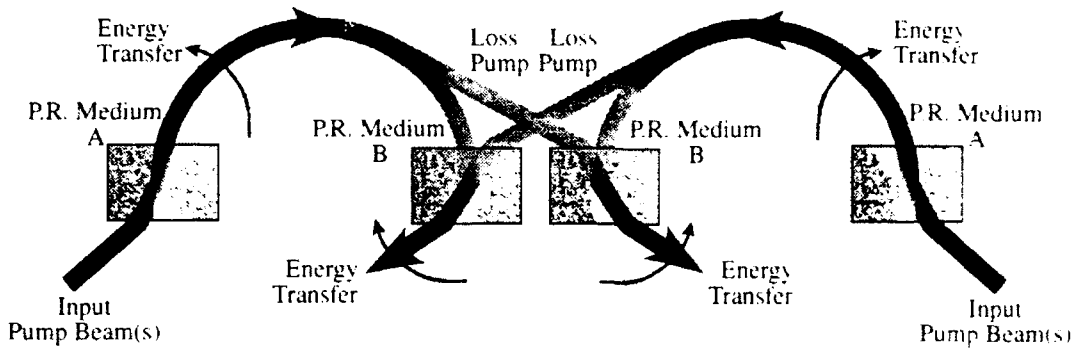

Figure II.1 The photorefractive flip-flop

There is also a matrix $\hat{T}^{(3)}$ describing the propagation of perturbations when a pump beam interacts with two spatially uncorrelated signal fields.

With the help of these matrices the stability of very general photorefractive circuits may be analyzed. The details turn out to be lengthy and only a summary of the physical implications is given below.

The photorefractive flip-flop is shown in Fig. II.1 [4]. Conditions for existence of spatial bistability based on steady state considerations were given in [4]. This analysis also shows the effect of varying the crystal time constants. The flip-flop has six steady states: both rings off, one ring on and the other ring off, both rings on equally and both rings on with unequal intensities. It turns out that all the stationary states, including the flip-flop state, are unstable when $\tau_L >> \tau_G$. So it is necessary to have a fast loss crystal, for the flip-flop to be stable. The same type of constraint applies in e.g., the bistable ring resonator [1,2] where the off state is unstable when the loss mechanism is too slow.

A slightly different configuration where the two rings share a common gain volume has also been analyzed. The shared volume leads to additional competition between the rings and the flip-flop state is now stable, while all other states are unstable, when $\tau_L >> \tau_G$. The experimental realization of the flip-flop [4] resulted in partial sharing of the gain volume between the rings, and had $\tau_L > \tau_G$.

A simplified model of the self-organizing feature extractor based on two coupled single-mode photorefractive ring oscillators is shown in Fig. II.2. The device that was experimentally demonstrated was based on two coupled multi-mode resonators, each containing an additional photorefractive crystal that ensured that the multi-mode ring behaved as though it were a single mode ring. In order to make the problem analytically tractable each multi-mode ring with its extra photorefractive crystal is modeled as an empty single mode ring. The set of equations

$$\frac{\partial s_{jk}}{\partial z} = \sum_{i=1}^{2} g_{ij} p_{ik}, \qquad \frac{\partial p_{jk}}{\partial z} = -\sum_{i=1}^{2} g_{ij} s_{ik},$$

$$\tau \frac{\partial g_{ij}}{\partial t} + g_{ij} = \frac{\Gamma}{2I_T} \sum_{k=1}^{2} s_{ik} p_{jk}^{*}, \qquad \text{(II.6)}$$

$$\tau = \tau_0 / I_T, \qquad I_T = \sum_{ij} \left(s_{ij}^2 + p_{ij}^2 \right)$$

captures the essential dynamics of this system. In (II.6) s_{ik} is the field amplitude of

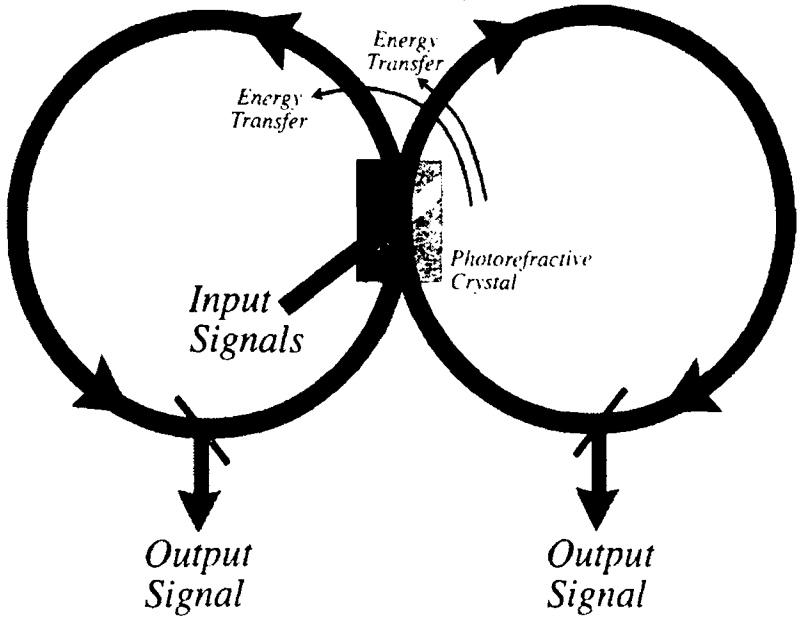

Figure II.2 Simplified model of a photorefractive feature extractor consisting of two single-mode resonators with shared gain volume.

signal k in ring i, p_{jk} is the field amplitude of the input pump beam in spatial mode j and temporal mode k, g_{ik} is the refractive index grating coupling ring i to pump spatial mode k, τ is the photorefractive time constant and I_T is the total optical intensity.

These equations are supplemented by the boundary conditions

$$p_{11}(z=0,t) = p_{011}, \qquad p_{22}(z=0,t) = p_{022}, \qquad p_{12}(z=0,t) = p_{21}(z=0,t) = 0$$

$$s_{11}(0,t) = e^{-C_1/2} s_{11}(l,t), \qquad s_{12}(0,t) = e^{-C_1/2} s_{12}(l,t), \quad g_{ij}(z,0) = 0. \qquad \text{(II.7)}$$

Here $e^{-C_i/2}$ is the reflectivity of ring i and the photorefractive medium has length l.

We wish to examine the stability of the stationary states of this system when it is driven by two spatio-temporally distinct signals with similar input intensities. There are four cases to consider: 1) there is no oscillation, 2) one of the input signals oscillates in one ring, 3) one input signal oscillates in both rings, and 4) one input signal oscillates in one ring and the other input signal oscillates in the other ring. The possibility of two input signals oscillating in a single ring need not be considered since analysis of a single ring resonator pumped by two input signals shows that the only stationary state corresponds to the stronger input signal oscillating, with the weaker input

signal completely suppressed. (In the degenerate case where the two inputs have the same intensity a linear combination of both signals may oscillate.)

The details of the linear stability analysis are rather lengthy [8]. It is found that the only stable solution is the desired state where one signal oscillates in one ring, and the other signal oscillates in the other ring. This is a stable state, provided the overall gain puts the circuit above threshold, as long as the larger input signal picks the ring with lower losses. Otherwise the signals simply switch rings. The degenerate case where the input signals have equal intensity [29], and the two rings have equal losses is somewhat arbitrary since there is a family of stable solutions described by $s_{12}/s_{11} = -s_{21}/s_{22} = const.$ Numerical studies of the full time dependent set of equations verify that when random noise is added to the input signals the resulting values of c are uniformly distributed.

III. Spatio-temporal dynamics in photorefractive ring oscillators

The self-imaging ring resonator is a highly degenerate device. Since any transverse electric field profile, neglecting diffraction, is imaged onto itself after one round trip the eigenmodes of the empty cavity form a continuous set. In this situation, where the passive optics play only a minor role in determining the mode structure, the impact of the nonlinear elements comes to the forefront. The self-imaging ring is therefore an interesting test bed, both for studying the effects of nonlinearity, and for learning how to use nonlinearity to control the spatio-temporal behavior in the resonator.

The single transverse mode ring resonator with photorefractive gain and loss has been shown to exhibit bistability and self-pulsing [1,2]. The interesting dynamical behavior in

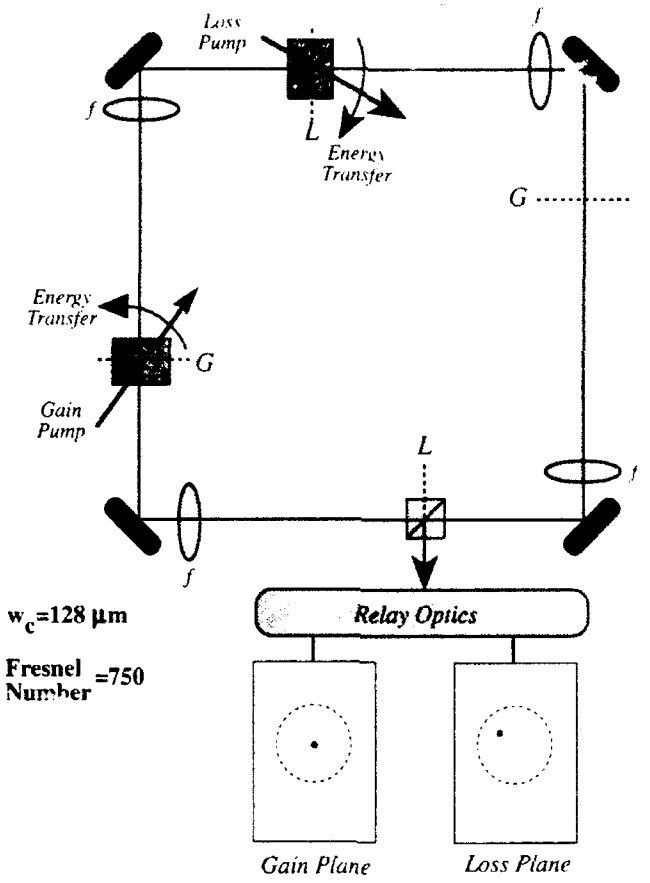

Fig. III.1 Imaging ring resonator with photorefractive gain and loss. All lenses are f=100 mm with a spacing of 2f. The gain and loss pumps are from a cw Argon laser, λ=514 nm.

this system is due to the competitive interaction of the gain and the loss. On the other hand, in the imaging resonator with a continuum of transverse modes, (see Fig. III.1) the interaction of the gain and the loss assumes a cooperative character in the following sense. Consider first what happens when only the gain pump is turned on. If the gain pump has a Gaussian profile then the oscillating mode will also assume a Gaussian profile, in the gain crystal, in order to maximize its overlap with the gain pump. However, the phase of the oscillating mode is unconstrained since it has no effect on the energy transfer efficiency in the gain medium. The Fourier transform of a field with Gaussian intensity profile but random phase is a rather random looking pattern. Now turn on the loss pump that interacts with this random pattern. When the random pattern contracts to a localized mode it maximizes its peak intensity and saturates the loss mechanism. There is a limit to how far the mode will contract, since if it becomes too small its Fourier transform will become too big and no longer be optimally matched to the gain pump in the conjugate plane. Thus, if the gain pump is a Gaussian with spot size w_c, where $w_c = \sqrt{\lambda f/\pi}$ is the confocal mode size of the passive cavity, and the loss pump is somewhat larger and transversely uniform then the gain and the loss interactions will

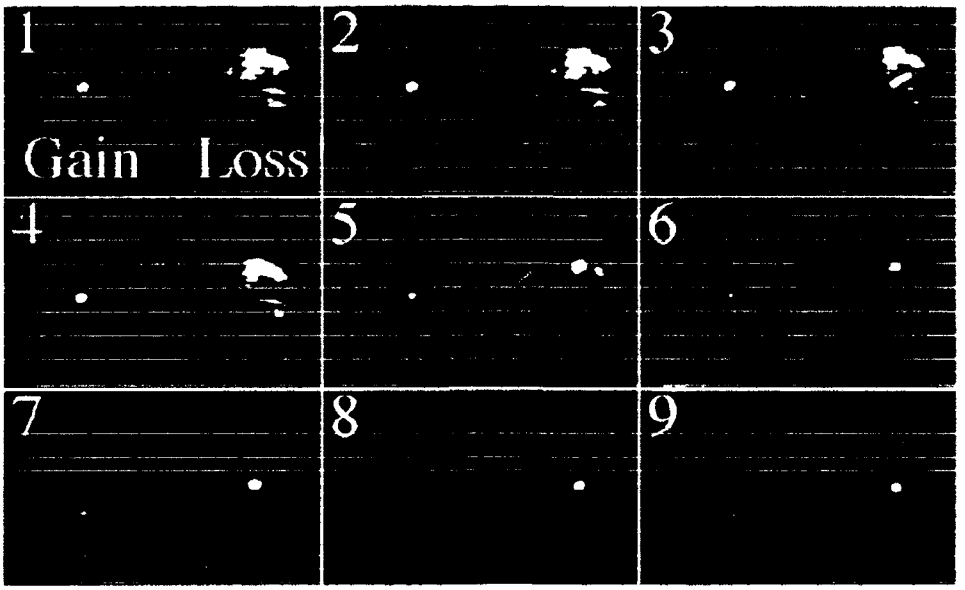

Fig. III.2. Collapse of the transverse mode structure. The first frame shows the mode profile immediately before the loss pump is turned on. The following frames are separated by 1/30 sec., with the gain plane on the left and the loss plane on the right.

cooperate spatially to from an oscillating mode with Gaussian spot size w_0, but arbitrary location in the plane of the loss interaction. An experimental recording of this effect is shown in Fig. III.2 [9].

However, once the mode profile has collapsed it begins to wander about in the transverse plane [10]. An example of this motion is shown in Fig. III.3. Depending on the details of the cavity alignment, and the gain and loss pump intensities, the spot either drifts to the edge of the available aperture and disappears before reappearing again in its original position, or else it executes a cyclic motion wholly within the aperture. In the latter case the spot does not move in a closed circle but rather appears, moves a short distance, and then disappears, before repeating its motion. It takes a few seconds for the spot to execute a single traverse across the aperture. The spot will typically choose a new drift path after about 10 cycles along any given path. The wandering motion, alternating between paths that are each repeated a few times, continues indefinitely. The spot motion appears to be determined by the cavity alignment since small adjustments to one of the resonator mirrors change the spot trajectory noticeably.

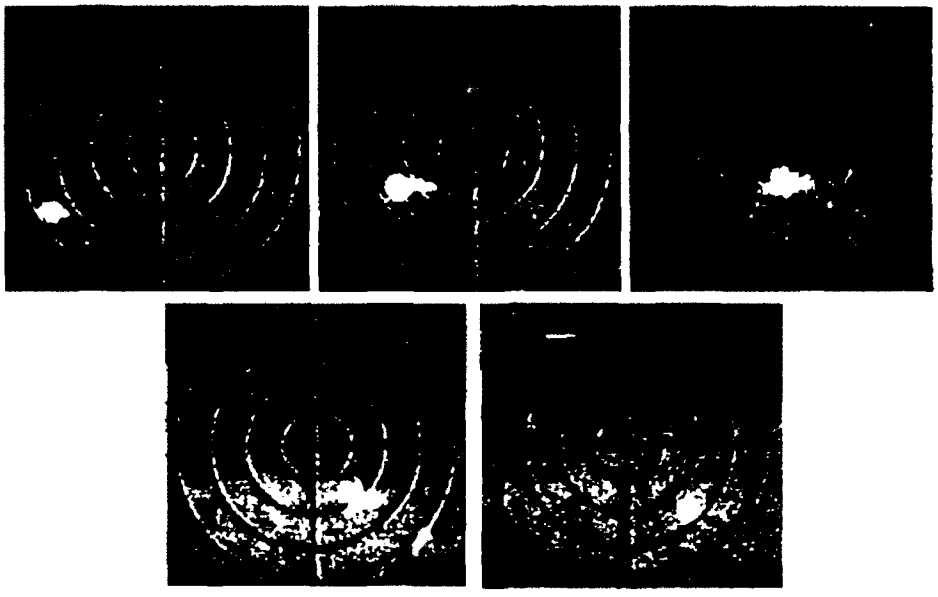

Fig. III.3. Experimental observation of spot motion. The frames were recorded at 0, 3, 7, 9 and 10 seconds of elapsed time, starting at the upper left and ending at the lower right.

The spot motion has been simulated by numerical calculations of the resonator dynamics [21]. The optical field and the photorefractive gratings are discretized on a square lattice. We assume no crossing of the pump and signal beams in the gain or loss crystals, but retain the axial dependence of the field and gratings in each crystal. Thus there is no nonlocal coupling within the crystals. The transverse coupling which leads to mode collapse arises from placing the crystals in spatially conjugate planes. If the cavity is assumed to be perfectly aligned the spot forms in a location determined by the maximum of the initial seeding, and is stationary. Misalignment of the cavity is modeled by introducing a phase wedge in the cavity $\Phi(x,y) = \exp i(\delta_x x + \delta_y y)$, where x, y are the transverse coordinates and δ_x, δ_y characterize the slope of the wedge. Placing the wedge next to the gain crystal results in a continuous motion of the spot parallel to the wedge gradient $\nabla\Phi \sim \delta_x \hat{x} + \delta_y \hat{y}$. An analytical study of the spot motion [21] for the case of one transverse dimension predicts that for small cavity misalignment the drift rate is

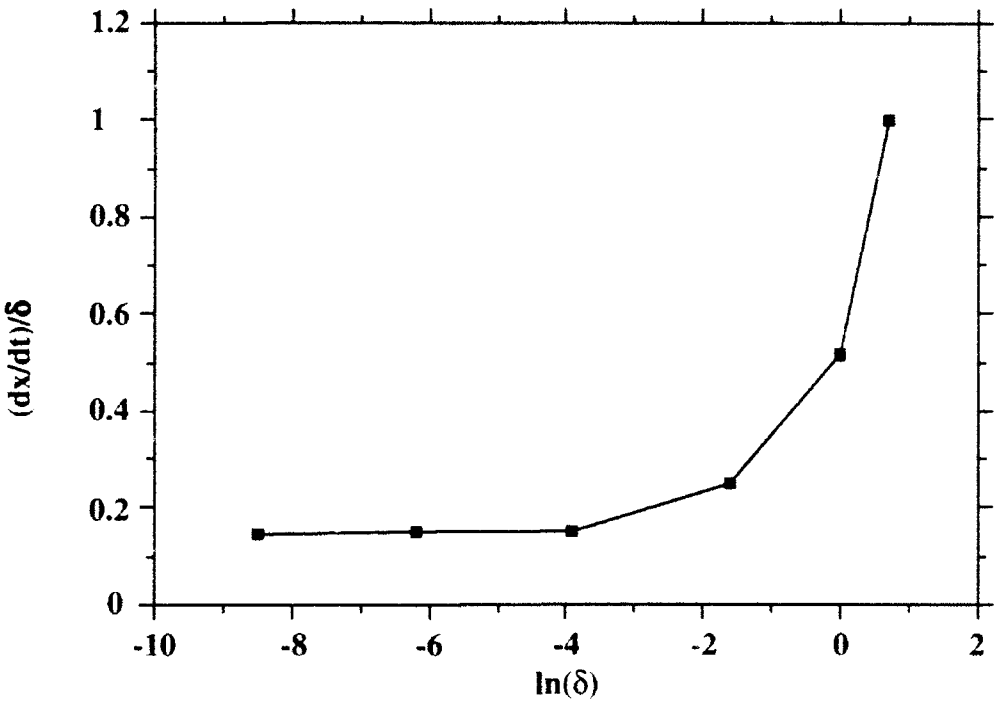

Figure III.4 Rate of spot motion vs. cavity misalignment as calculated by direct numerical simulation. For small δ the rate depends linearly on δ. The actual rate agrees with Eq.(III.1) to within about 30%, depending on the values of the resonator parameters.

$$\frac{dx}{dt} = \frac{f}{k}\frac{\delta}{\tau \ln\left(I_p / I_{osc}\right)}, \qquad \text{(III.1)}$$

where x is the position of the spot in the loss plane, τ is the time constant of the gain medium, I_p is the maximum pump beam intensity and I_{osc} is the maximum oscillating intensity at the entrance to the gain medium. In deriving Eq. (III.1) the time constant of the loss crystal has been put to zero. In the actual experiment the time constant of the loss crystal was approximately 20 times shorter than that of the gain crystal, so this is a reasonable approximation. Comparison of Eq. (III.1) with the drift rate found from direct numerical simulations is shown in Fig. III.4. The drift rate is indeed linearly proportional to δ for small δ. It is surprising how small δ must be before a linear dependence of drift rate on cavity misalignment is obtained. This indicates that a higher order theory, which allows for a nonlinear dependence on δ may be necessary to get good agreement between the analytical and numerical descriptions.

It appears clear from the analytical and numerical studies that the motion of the localized mode is a direct consequence of cavity misalignment. Even if the misalignment is made very small the spot will continue to move, albeit slowly. In order to use this type of resonator for implementation of a neuromorphic optical processor we wish to eliminate the spot motion. We have very recently found a configuration involving a resonator with three photorefractive crystals that eliminates the spot motion in our computer simulations. On going work will concentrate on experimental verification and analytical study of this new configuration.

IV. Transverse instability of counterpropagating beams

Transverse modulational instability of two counterpropagating beams in nonlinear optical media has been observed in atomic vapors [13-15], liquid crystals [16,17], and quite recently in photorefractive crystals [18]. The instability manifests itself in the far field by the appearance of conical rings, pairs of spots or a hexagonal array of spots about the counterpropagating beams. The corresponding intensity modulation in the near field has the characteristic spatial scale $l_t = 2\pi/\theta_t k_0$, where θ_t is the small angle between the generated satellite beams and the primary beams. The angle θ_t at which the threshold of the absolute instability is a minimum may be found for all of the above materials by a linearized analysis of the equations of motion [12,19,20,22-26]. On the other hand, the nature of the nonlinear stage of the instability, the details of the resulting patterns, and their spatial and temporal stability appear to vary widely among different materials. In atomic vapors, cones, pairs of spots and hexagons may all be observed depending on the frequency and intensity of the primary beams. In liquid crystals the instability leads to a stable hexagonal pattern, whereas the recent observations in photorefractive media indicate a somewhat different behavior. Here the hexagonal pattern is well defined, but temporally and spatially unstable, such that it appears as a cone in a time averaged recording. The cones observed in atomic vapors may also be due to unstable hexagons although no time resolved data is presently available. There is some reason to expect this since, as was shown in [15], the cone may be collapsed into a hexagon by injection of a weak beam at θ_t.

Although the general nature of the instability in photorefractive media is similar to the well known Kerr nonlinearity case, the details of the instability threshold conditions differ. This is due to several differences between the photorefractive and Kerr-type nonlinearities. In Kerr-type media the nonlinear part of the refractive index n is not (or is only weakly) dependent on the angle θ between the interacting waves (see Fig. IV.1) or, equivalently, on the wavevector $k_t = \theta k_0$ of the grating written by the pumping waves with their sidebands (F_0 with F_{-1} and B_0 with B_{-1}) and so the characteristic angle θ_t is the result of interplay between the Kerr nonlinearity and diffraction. The nonlinear coupling coefficient (analog of n_2) in photorefractive media is strongly dependent on the value of k_t and so material properties of the crystal must come into play, imposing their own characteristic spatial scales. Furthermore, the Kerr nonlinearity corresponds to a

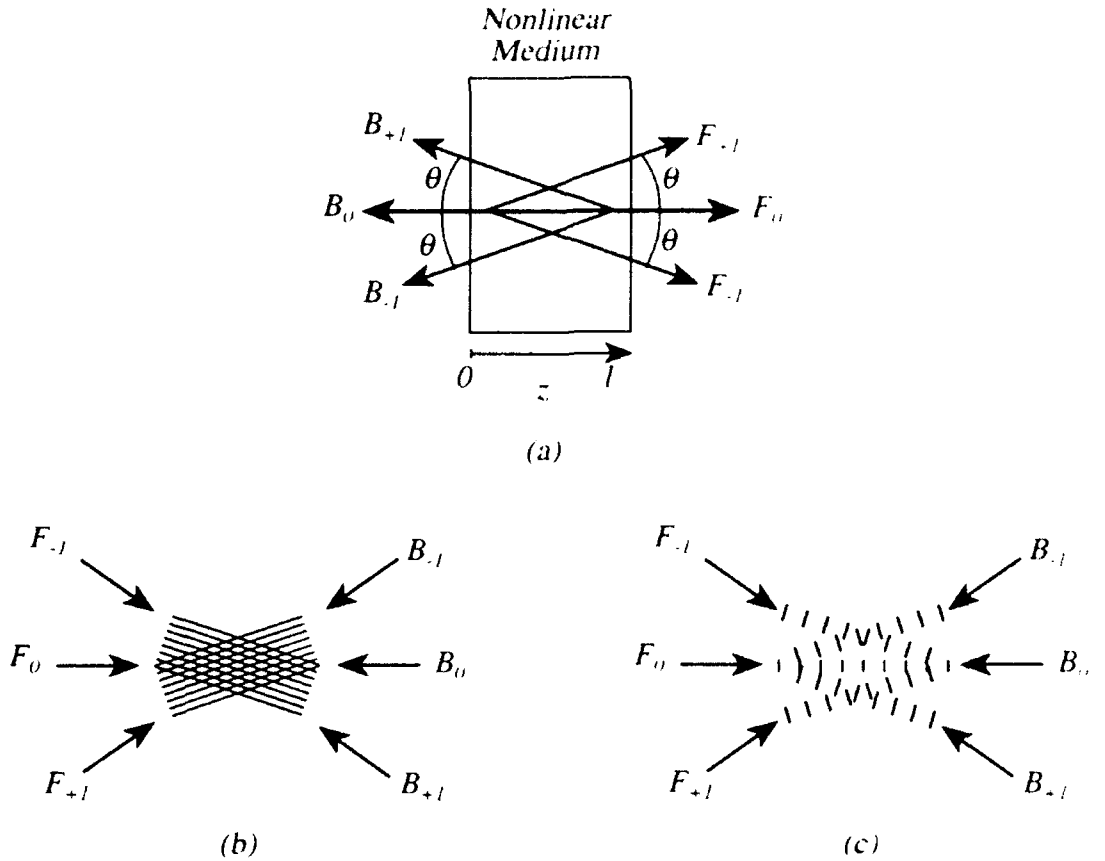

Figure IV.1. Transverse instability of counterpropagating beams. a) Geometry of the optical interaction: (F_0, B_0) are the incident pump beams while $(F_{\pm 1}, B_{\pm 1})$ are spontaneously generated satellites b) transmission gratings couple the beam pairs $\{(F_0, F_{+1}), (B_0, B_{-1})\}$, and $\{(F_0, F_{-1}), (B_0, B_{+1})\}$, and c) reflection gratings couple the beam pairs (F_0, B_0), $\{(F_0, B_{-1}), (F_{-1}, B_0)\}$, and $\{(F_0, B_{+1}), (F_{-1}, B_0)\}$.

nonlinear change of phase (n_2 is purely real) whereas the photorefractive nonlinearity is in general complex corresponding to both amplitude and phase changes. The magnitude of the real part of the coupling coefficient can be enhanced by applying an external electric field to the photorefractive crystal, but in general it is impossible to completely eliminate the imaginary part. Also the dependence of the real and imaginary parts on the value of $k_\perp$ is different. In addition photorefractive media are characterized by strong amplified incoherent scattering (fanning) which leads to a dependence of the amplitudes of the primary beams on the axial coordinate, even in the linear stage of the instability.

The details of the analysis in photorefractive media depend on whether the instability is due to the formation of transmission or reflection gratings. The interacting waves are written in the form

$$F(\vec{r}_\perp, z, t) = F_0(z)[1 + F_{+1}\exp(i\vec{k}_\perp \vec{r}_\perp - i\Omega t) + F_{-1}\exp(-i\vec{k}_\perp \vec{r}_\perp + i\Omega^* t)]\exp(ik_0 z - i\omega_0 t),$$
$$B(\vec{r}_\perp, z, t) = B_0(z)[1 + B_{+1}\exp(i\vec{k}_\perp \vec{r}_\perp - i\Omega t) + B_{-1}\exp(-i\vec{k}_\perp \vec{r}_\perp + i\Omega^* t)]\exp(-ik_0 z - i\omega_0 t) \quad \text{(IV.1)}$$

which leads to the equations of motion

$$
\begin{aligned}
(\partial/\partial z + ik_d)F_{+1} &= i\frac{\gamma}{1+q}\left[F_{+1} + F_{-1}^{*} + q(B_{+1} + B_{-1}^{*})\right], \\
(\partial/\partial z - ik_d)F_{-1}^{*} &= -i\frac{\gamma}{1+q}\left[F_{+1} + F_{-1}^{*} + q(B_{+1} + B_{-1}^{*})\right], \\
(\partial/\partial z - ik_d)B_{+1} &= -i\frac{\gamma}{1+q}\left[F_{+1} + F_{-1}^{*} + q(B_{+1} + B_{-1}^{*})\right], \\
(\partial/\partial z + ik_d)B_{-1}^{*} &= i\frac{\gamma}{1+q}\left[F_{+1} + F_{-1}^{*} + q(B_{+1} + B_{-1}^{*})\right]
\end{aligned}
\qquad \text{(IV.2)}
$$

for transmission gratings and

$$
\begin{aligned}
\frac{\partial F_0}{\partial z} &= i\gamma\frac{q}{1+q}F_0, \\
\frac{\partial B_0}{\partial z} &= -i\gamma^{*}\frac{1}{1+q}B_0, \\
(\partial/\partial z + ik_d)F_{+1} &= i\frac{q}{1+q}\left[(\gamma^{+} - \gamma)F_{+1} + \gamma B_{+1} + \gamma^{+}B_{-1}^{*}\right], \\
(\partial/\partial z - ik_d)F_{-1}^{*} &= -i\frac{q}{1+q}\left[(\gamma^{-*} - \gamma^{*})F_{-1}^{*} + \gamma^{-*}B_{+1} + \gamma^{*}B_{-1}^{*}\right], \\
(\partial/\partial z - ik_d)B_{+1} &= -i\frac{1}{1+q}\left[\gamma^{*}F_{+1} + \gamma^{-*}F_{-1}^{*} + (\gamma^{-*} - \gamma^{*})B_{+1}\right], \\
(\partial/\partial z + ik_d)B_{-1}^{*} &= i\frac{1}{1+q}\left[\gamma^{*}F_{+1} + \gamma F_{-1}^{*} + (\gamma^{+} - \gamma)B_{-1}^{*}\right].
\end{aligned}
\qquad \text{(IV.3)}
$$

for reflection gratings. In Eqs. (IV.2) $q(z) = |B_0(z)/F_0(z)|^2$, $k_d = k_\perp^2/2k_0$, and $\gamma(\bar{k}_\perp, \Omega)$ is the material and frequency shift dependent complex coupling coefficient. In (IV.3) $\gamma \equiv \gamma(2\bar{k}_0, \Omega = 0)$ and $\gamma^{\pm} = \gamma/1 \mp \Omega\tau$.

The dispersion relationship governing the instability threshold is found by solving Eqs. (IV.2, IV.3) with the boundary conditions $F_{+1}(z=0) = F_{-1}(0) = 0$, $B_{+1}(z=l) = B_{-1}(l) = 0$. In the case of transmission gratings Eqs.(IV.2) may be solved in closed form for arbitrary axial variation of $q(z)$ We find that the dispersion relation is given by

$$(1-A_1)(1-A_2)-A_3A_4=0,$$

$$A_1=(2\gamma k_d/s)\int_0^l dz\,\frac{q(z)}{1+q(z)}\,\frac{\sin(k_d z)}{\sin(k_d l)}\sinh[s(z-l)],$$

$$A_2=(2\gamma k_d/s)\int_0^l dz\,\frac{1}{1+q(z)}\,\frac{\sin[k_d(z-l)]}{\sin(k_d l)}\sinh(sz),$$

$$A_3=(2\gamma k_d/s)\int_0^l dz\,\frac{q(z)}{1+q(z)}\,\frac{\sin[k_d(z-l)]}{\sin(k_d l)}\sinh[s(z-l)],$$

$$A_4=(2\gamma k_d/s)\int_0^l dz\,\frac{1}{1+q(z)}\,\frac{\sin(k_d z)}{\sin(k_d l)}\sinh(sz),$$

$$s=\left[k_d(2\gamma-k_d)\right]^{1/2} \qquad \text{(IV.4)}$$

For $q=const.$ Eqs. (IV.4) reduces to

$$\left(q+q^{-1}\right)+\left[(s/k_d)^{-1}-(s/k_d)\right]\sin(k_d l)\sinh(sl)+2\cos(k_d l)\cosh(sl)=0. \qquad \text{(IV.5)}$$

If we impose the restriction of purely real γ and $\Omega=0$ this equation corresponds to the known results for Kerr media [12,22-26].

Several of the lowest branches found from numerical solution of Eq. (IV.5) are shown in Fig. IV.2. Taking $q=const.$ is usually not a good approximation in photorefractive media due to the influence of passive absorption, and beam fanning. The amount of beam fanning may be reduced by working with narrow beams, although in the transmission grating geometry the beam diameter cannot be made too small due to the requirement of having at least a few modulation fringes across the main beams. Numerical solution of Eqs. (IV.4) with $q(z)=q(0)e^{2\alpha_{eff}z}$, where $\alpha_{eff}=9cm^{-1}$ accounts for passive absorption and fanning as measured with mm sized beams in a piece of $BaTiO_3$, shows that the

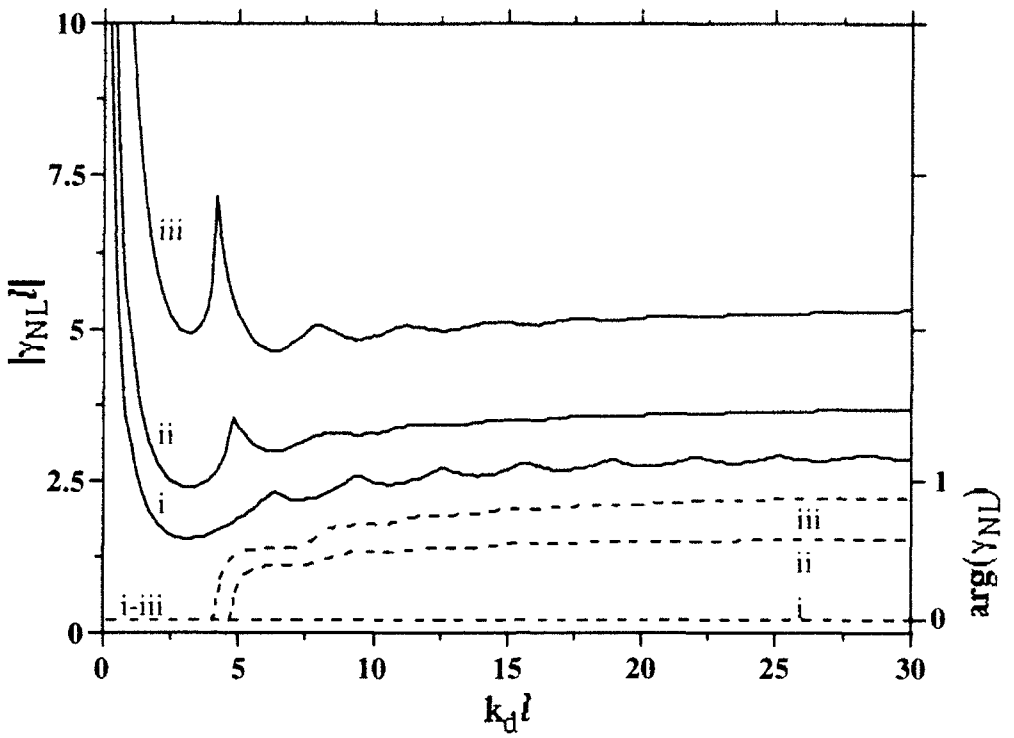

Fig. IV.2. Dispersion curves for q(z)=const.: a) focusing branch with $\mathrm{Re}(\gamma) > 0$ and b) defocusing branch with $\mathrm{Re}(\gamma) < 0$. The curves are labeled as i) q=1, ii) q=10, and iii) q=100. —— $|\gamma|$, - - - - $\arg(\gamma)$.

necessary coupling constant for observation of instabilities is increased by about a factor of 5.

The recent experimental observation of the modulational instability in photorefractive media[18] used a reflection grating geometry. This is advantageous since it is then possible to use very narrow beams, which reduces fanning losses. Eqs. (IV.3) describing the reflection grating case are more complex than those describing transmission gratings and general solutions for $q = q(z)$ are not available. However, by choosing the boundary conditions such that $|F_0(l)|^2 = |B_0(l)|^2$ results in $q = 1$ throughout the photorefractive medium since Eqs. (IV.3) have the first integral $|F_0(l)|^2 - |B_0(l)|^2 = const.$ for any value of γ. Putting $q = 1$ in Eqs. (IV.3) results in the dispersion relationship

$$\cosh\left(\frac{\gamma_r l}{1 - i\Omega\tau}\right) + \cos(s^0 l)\cos(sl) + \frac{1}{s^0 s}\left[\left(k_d + \frac{\gamma_r}{2}\right)\left(k_d + \frac{\gamma_r}{2}\left(1 - \frac{2}{1 - i\Omega\tau}\right)\right) + \frac{|\gamma|^2}{4}\right]\sin(s^0 l)\sin(sl) = 0. \tag{IV.6}$$

where $s^{0^2} = (k_d + \gamma_r/2)^2 - |\gamma|^2/4$ and $s^2 = \left(k_d + \frac{\gamma_r}{2}\left(1 - \frac{2}{1 - i\Omega\tau}\right)\right)^2 - |\gamma|^2/4$. This equation is different from those derived previously for Kerr media since it includes the redistribution of energy between the counterpropagating pump beams due to the formation of reflection gratings. Numerical evaluation of the threshold condition predicted by this equation is in progress [20].

References

1. D. M. Lininger, P. J. Martin, and D. Z. Anderson, "Bistable ring resonator utilizing saturable photorefractive gain and loss," Opt. Lett. **14**, 697 (1989).

2. D. M. Lininger, D. D. Crouch, P. J. Martin, and D. Z. Anderson, "Theory of bistability and self pulsing in a ring resonator with saturable photorefractive gain and loss," Opt. Commun. **76**, 89 (1990).

3. C. Benkert and D. Z. Anderson, "Controlled competitive dynamics in a photorefractive ring oscillator: 'Winner-takes-all' and the 'voting-paradox' dynamics," Phys. Rev. A **44**, 4633 (1991).

4. D. Z. Anderson, C. Benkert, B. Chorbajian, and A. Hermanns, "Photorefractive flip-flop," Opt. Lett. **16**, 250 (1991).

5. D. D. Crouch and D. Z. Anderson, "Dynamics of an optical ring circuit having photorefractive gain and loss and history-dependent feedback," J.O.S.A. B **8**, 1315 (1991).

6. M. Saffman, C. Benkert, and D. Z. Anderson, "Self-organizing photorefractive frequency demultiplexer," Opt. Lett. **16**, 1993 (1991).

7. D. Z. Anderson, C. Benkert, V. Hebler, J.-S. Jang, D. Montgomery, and M. Saffman, "Optical implementation of a self-organizing feature extractor," in Advances in Neural-Information Processing Systems IV, ed. J. E. Moody, S. J. Hanson, and R. P. Lippmann, (Morgan Kaufmann, San Mateo, 1992), p. 821-828.

8. M. Saffman, D. Montgomery, A. A. Zozulya, and D. Z. Anderson, "Self-Organization and learning in photorefractive ring oscillators," to be submitted.

9. M. Saffman, D. Montgomery, and D. Z. Anderson, "Collapse of a transverse mode continuum in a photorefractive oscillator," in Nonlinear Dynamics in Optical Systems Technical Digest, 1992 (Optical Society of America, Washington, DC., 1992), Vol. 16.

10. M. Saffman, D. Montgomery, A. A. Zozulya, and D. Z. Anderson, "Wandering excitations in a photorefractive ring resonator," to be presented at the topical meeting on Photorefractive Materials, Effects, and Devices, Kiev, 1993.

11. T. Kohonen, *Self-Organization and Associative Memory, 3rd ed.* , (Springer-Verlag, Berlin, 1989).

12. S. N. Vlasov and V. I. Talanov, in Optical Phase Conjugation in Nonlinear Media, V. I. Bespalov ed., p.85, (Inst. of Applied Physics, USSR Academy of Sciences, Gorki, 1979).

13. G. Grynberg, E. Le Bihan, P. Verkerk, P. Simoneau, J. R. R. Leite, D. Bloch, S. Le Boiteux and M. Ducloy, "Observation of instabilities due to mirrorless four-wave mixing oscillation in sodium," Opt. Commun. **67**, 363 (1988).

14. A. Petrossian, M. Pinard, A. Maître, J.-Y. Courtois and G. Grynberg, "Transverse-pattern formation for counterpropagating beams in rubidium vapor," Europhys. Lett. **18**, 689 (1992).

15. J. Pender and L. Hesselink, "Conical emissions and phase conjugation in atomic sodium vapor," IEEE J.Q.E. **25**, 395 (1989); J. Pender and L. Hesselink, "Degenerate conical emission in atomic-sodium vapor," J.O.S.A. B **7**, 1361 (1990).

16. R. Macdonald and H. J. Eichler, "Spontaneous optical pattern formation in a nematic liquid crystal with feedback mirror," Opt. Commun. **89**, 289 (1992).

17. M. Tamburrini, M. Bonavita, S. Wabnitz, and E. Santamato, "Hexagonally patterned beam filamentation in a thin liquid-crystal film with a single feedback mirror," Opt. Lett. **18**, 855 (1993).

18. T. Honda, "Hexagonal pattern formation due to counterpropagation in $KNbO_3$," Opt. Lett. **18**, 598 (1993).

19. M. Saffman, D. Montgomery, A. A. Zozulya, K. Kuroda, and D. Z. Anderson, "Transverse instability of counterpropagating waves in photorefractive media," to appear in Phys. Rev. A.

20. M. Saffman, A. A. Zozulya, and D. Z. Anderson, "Transverse instability of counterpropagating waves in photorefractive media with energy transfer between the pump waves," in preparation.

21. M. Saffman, A. A. Zozulya, D. Montgomery, and D. Z. Anderson, "Spatio-temporal dynamics of localized excitations in a photorefractive ring resonator," in preparation, will appear in a forthcoming special issue of Chaos, Solitons and Fractals, (1994).

22. S. N. Vlasov and E. V. Sheinina, "On the theory of interaction of counterpropagating waves in a nonlinear cubic medium," Izv. Vyssh. Ucebn. Zaved. Radiofiz. **26**, 20 (1983) [Radiophys. Quant. Electron. **27**, 15 (1983)].

23. W. J. Firth and C. Paré, "Transverse modulational instabilities for counterpropagating beams in Kerr media," Opt. Lett. **13**, 1096 (1988).

24. G. Grynberg and J. Paye, "Spatial instability for a standing wave in a nonlinear medium," Europhys. Lett. **8**, 29 (1989).

25. W. J. Firth, A. Fitzgerald and C. Paré, "Transverse instabilities due to counterpropagation in Kerr media," J.O.S.A. B **7**, 1087 (1990).

26. G. G. Luther and C. J. McKinstrie, "Transverse modulational instability of counterpropagating light waves," J.O.S.A. B **9**, 1047 (1992).

27. A. A. Zozulya and D. Z. Anderson, "Theoretical analysis of a photorefractive flip-flop," to be submitted.

28. A. A. Zozulya and V. T. Tikhonchuk, "Investigation of stability of four-wave mixing in photorefractive media," Phys. Lett. A **135**, 447 (1989).

29. D. Z. Anderson, M. Saffman, and A. Hermanns, "Manipulating the information carried by an optical beam with reflexive photorefractive beam coupling," to be submitted.